

Energy Interplay in Materials: Unlocking Next-Generation Synchronous Multisource Energy Conversion with Layered 2D Crystals

Alexander Corletto, Amanda V. Ellis,* Nick A. Shepelin, Marco Fronzi, David A. Winkler, Joseph G. Shapter, and Peter C. Sherrell*

Layered 2D crystals have unique properties and rich chemical and electronic diversity, with over 6000 2D crystals known and, in principle, millions of different stacked hybrid 2D crystals accessible. This diversity provides unique combinations of properties that can profoundly affect the future of energy conversion and harvesting devices. Notably, this includes catalysts, photovoltaics, superconductors, solar-fuel generators, and piezoelectric devices that will receive broad commercial uptake in the near future. However, the unique properties of layered 2D crystals are not limited to individual applications and they can achieve exceptional performance in multiple energy conversion applications synchronously. This synchronous multisource energy conversion (SMEC) has yet to be fully realized but offers a real game-changer in how devices will be produced and utilized in the future. This perspective highlights the energy interplay in materials and its impact on energy conversion, how SMEC devices can be realized, particularly through layered 2D crystals, and provides a vision of the future of effective environmental energy harvesting devices with layered 2D crystals.

components of the green energy revolution. Although medium to large devices, such as silicon solar cells, have revolutionized energy generation, small-scale and personal devices remain impractical.^[1] This lack of small energy harvesting devices in the market is due to the relatively small amount of energy such devices may capture, and the losses in extracting the energy (power management) from the device for use. Indeed, indoor light-harvesting has three orders of magnitude less available energy compared to outdoor light-harvesting (Table 1).^[2] While the losses in extracting energy can be improved by optimizing the materials' interfaces and electronic circuitry, the amount of energy available to harvest is limited. Thus, to provide higher energy and power output, small-scale energy harvesters must be found that increase utilization of the total available environmental energy.

1. Introduction

Energy harvesting and conversion systems that take ambient energy from the environment to generate electricity are critical

Traditional energy harvesters have focused on single energy sources including mechanical (force^[3,4] and friction^{[5]), electro-magnetic (light and magnets^{[6]), or thermal energy, and huge advances have been made in improving their efficiencies.}}

A. Corletto, A. V. Ellis, P. C. Sherrell
Department of Chemical Engineering
The University of Melbourne
Grattan Street, Parkville, Victoria 3010, Australia
E-mail: amanda.ellis@unimelb.edu.au; peter.sherrell@unimelb.edu.au

N. A. Shepelin
Laboratory for Multiscale Materials Experiments
Paul Scherrer Institute
Forschungsstrasse 111, Villigen CH-5232, Switzerland


M. Fronzi
School of Mathematical and Physical Science
University of Technology Sydney
Ultimo, New South Wales 2007, Australia

D. A. Winkler
Monash Institute of Pharmaceutical Sciences
Monash University
381 Royal Parade, Parkville, Victoria 3052, Australia

D. A. Winkler
School of Biochemistry and Chemistry
La Trobe Institute for Molecular Science
La Trobe University
Kingsbury Drive, Bundoora, Victoria 3086, Australia

D. A. Winkler
School of Pharmacy
The University of Nottingham
Nottingham NG7 2RD, UK

J. G. Shapter
Australian Institute for Bioengineering and Nanotechnology
The University of Queensland
Brisbane, Queensland 4072, Australia

 The ORCID identification number(s) for the author(s) of this article can be found under <https://doi.org/10.1002/adma.202203849>.

© 2022 The Authors. Advanced Materials published by Wiley-VCH GmbH. This is an open access article under the terms of the Creative Commons Attribution License, which permits use, distribution and reproduction in any medium, provided the original work is properly cited.

DOI: 10.1002/adma.202203849

Table 1. Comparison of energy harvesting technology. Adapted under the terms of the CC-BY Creative Commons Attribution 4.0 International license (<https://creativecommons.org/licenses/by/4.0/>).^[2] Copyright 2017, The Authors, published by SAGE Journals.

Energy input	Power density	Harvesting method	Typical applications
Mechanical (human motion)	4 $\mu\text{W cm}^{-3}$	Piezoelectric/electrostatic	Wearable electronics
Thermal (person)	60 $\mu\text{W cm}^{-2}$	Thermoelectric	Wearable electronics
Light (indoors)	100 $\mu\text{W cm}^{-3}$	Photovoltaic	Handheld/wearable electronics
Thermal (industrial)	10 mW cm^{-2}	Thermoelectric	Waste heat recycling
Light (outdoors)	100 mW cm^{-3}	Photovoltaic	Solar cells
Mechanical (machine motion)	800 mW cm^{-3}	Electromagnetic	Sensing/ambient vibrations

However, focusing on a single energy source means that much of the available energy for harvesting is ignored.

Thus, the path forward is not about simply trying to squeeze further efficiencies from existing highly optimized single energy source technologies. Rather, it is realizing synchronous multisource energy conversion (SMEC) from a single material; synchronously (simultaneously) converting multiple energy sources into useable electrical energy without subtractive effects.^[7,8] Employing SMEC materials in energy harvesting devices would allow the devices to harvest energy from heat energy (e.g., body heat, solar heat, and engine heat), light energy (e.g., sunlight and ambient light), and mechanical energy (e.g., body movement and machine/ambient vibrations) at the same time, and in one material and device. However, in the literature, multiple energy conversion mechanisms are often described as decoupled effects, where a single energy conversion mechanism of a material or system is explored, rather than acknowledging measured voltages, deformations, currents, or photoemissions can arise from many energy conversion mechanisms occurring simultaneously or in quick succession. This lack of consideration of multiple simultaneous conversions has likely occurred because few materials can effectively synchronously harvest multiple energy sources.

Initial solutions to this problem have been to harvest energy asynchronously or harvest the same “class” of energy (mechanical, thermal, or photonic). The main emergent technologies are piezoelectric and triboelectric energy generators (P-TEGs),^[9–11] piezo-photonics (PPs),^[12] and piezo-catalysts (PCs).^[12–14] All approaches thus far either harvest the same energy source (e.g., P-TEGs harvest mechanical energy through two different mechanisms) or capture two energy sources separately and transfer electric charge between two materials (e.g., PP and PC rely on vibrational (mechanical) energy conversion of one material changing the band structure of a different material that is catalytic or photoactive). P-TEGs are therefore still fundamentally limited by the single energy input, while PPs and PCs are restricted by losses occurring when charge is transferred between materials.

To discover, or design, SMEC materials for multisource energy harvesting, two key problems must be solved: 1) identify appropriate materials that can interact with a variety of different energy sources; and 2) understand how different energy conversion mechanisms in materials spontaneously affect other energy conversion mechanisms occurring synchronously. Layered 2D crystals exhibit highly anisotropic electronic, thermal and mechanical properties due to their high

aspect ratio, and nanoscale layer thickness.^[15] The high aspect ratio enables macroscale surfaces to be covered in 2D materials, while maintaining the nanoscale quantum properties of crystals.^[16] In contrast to, for example, 1D or 0D materials systems, these macroscale surfaces can exist without disordered interfaces and pinholes, consequently enabling homogenous energy harvesting device performance. Finally, the planarity of layered 2D crystals, coupled with interlayer van der Waals (vdWs) stacking, enables new properties to be directly induced by the fabrication of 2D heterostructures.^[17] Conceptually, this allows the introduction of ferroelectric properties in thermoelectric, or photovoltaic 2D crystals, thus enabling SMEC in state-of-the-art energy harvesting and conversion systems. Layered 2D crystals are easier to synthesize and demonstrate improved stability in devices, in comparison to non-layered 2D crystals that possess high surface energies from dangling, unsaturated bonds.^[18,19] We propose that layered 2D crystals are therefore prime candidates for use as energy harvesting materials and, potentially, SMEC materials.

This perspective aims to provide a discussion around the following clear points. First, fundamental energy conversion in layered 2D crystals and their potential for energy harvesting are highlighted. Second, the energy interplay occurring within materials, the network of energy conversion mechanisms, and their effects on other energy conversion mechanisms occurring synchronously, are discussed. Finally, an outlook on the potential of layered 2D crystals, particularly ferroelectric 2D crystals, as SMEC materials and their use in SMEC devices is provided.

2. Properties of Layered 2D Crystals

Layered 2D crystals have unique and tunable optoelectronic properties due to their dimensionality.^[20] They typically also possess high mechanical strength and durability, ideal for small-scale or personal energy harvesting.^[20] This exceptionally chemically diverse class of materials, encompassing mono-elemental structures (e.g., graphene, antimonene, and silicene), chalcogenides (MX, MX₂, M₂X₃, MXY, MXY₂), MXenes (Ti₃C₂T_x), metal oxides (MO₂, MO₃, M₂O₃), and many more, can assemble via vdWs out of plane bonds to form heterostructures with unique properties.^[21] In particular, the formation of 2D crystal heterostructures and Janus 2D crystals (MXY or MXY₂)^[22–25] can allow the incorporation of additional energy conversion mechanisms (piezoelectricity, pyroelectricity, etc.) into these structures.^[17]

The nanometer-scale thickness of 2D crystals results in electrons behaving with reduced dimensionality under quantum confinement. This confinement reduces the phase space that electrons can populate in the material and consequently results in enhanced quantum effects, increased electron correlations, and altered electronic properties compared to bulk materials.^[26,27] These confinement effects are particularly maximized for isolated monolayer (single-atom/unit-cell-thick) crystals. Importantly, for energy conversion, the reduction in available phase space can drastically alter the electronic structure and bandgaps compared to bulk materials, and varies widely with the number of layers in the 2D crystals.^[26,28] A large range of electronic structures and bandgaps are therefore available that can be optimized for energy conversion devices. Additionally, the nanometer-scale thickness of 2D crystals minimizes the required conduction path to external interfaces resulting in reduced scattering and resistance, and minimizes electrical/magnetic field screening. These properties reduce losses in energy conversion mechanisms, manifested as a dramatically improved thermoelectric figure of merit (ZT) at the monolayer scale (Figure 1a),^[29] together with tunable light absorption across the electromagnetic spectra (Figure 1b).^[30] These unique properties make 2D crystals a prime candidate for energy conversion devices.

From the context of SMEC, layered 2D crystals have several key advantages over other systems. Notably, a high X,Y-Z aspect ratio in 2D crystals often exists with lateral size on the microscale, and thickness on the nanoscale. In contrast to 1D crystals, 2D crystals can cover surfaces without pinholes. This homogenous coating enables a large surface area for the capture of different energy inputs, an increased covered area for photon absorption, and greater contact area for thermal capture. In addition, the lack of dangling bonds in the Z-direction in layered 2D crystals enables vdWs 2D heterostructures to be fabricated that combine individual energy conversion mechanisms from each constituent crystal, thus generating a new SMEC system.

The following sections will delve into energy conversion in layered 2D crystals and discuss the interplay between different energy types.

3. Energy Conversion Mechanisms in Layered 2D Crystals

The discovery or design of SMEC materials for multisource energy harvesting requires a fundamental understanding of the driving forces for each energy conversion mechanism. The purpose here is not to delve deeply into every fundamental energy conversion mechanism, but to present the important energy conversion mechanisms and highlight the advantages of 2D crystals in these conversion mechanisms. In particular, the conversion of different energy sources into electrical energy is critical for advanced energy harvesting devices, as electrical energy is easily used and transmitted in most devices and is the focus of this perspective. Figure 2 shows the key energy sources for energy harvesting (mechanical (M), photonic (P), thermal (T)) and how these can interconvert and interact with each other and convert to useable electrical energy (E).

3.1. Mechano-Electrical (M → E) Energy Conversion in 2D Crystals

Conversion of mechanical energy to electrical energy (M → E) occurs through two primary mechanisms: 1) piezoelectricity, where mechanical stress is converted directly to charge; and 2) triboelectricity, where friction and motion between two materials induce charge separation.^[31] These processes find key applications in energy recovery systems in industry, wearable energy harvesters, and piezo-catalysis.

The key selection rule for the piezoelectric effect is an asymmetry in individual crystal unit cells. When the crystal is deformed, the asymmetry results in a change in the net dipole moment (i.e., polarization) of the crystal resulting in an induced charge on opposing parallel surfaces. While piezoelectricity is generally confined to non-centrosymmetric space groups, ferroelasticity and flexoelectricity can impart M → E energy conversion through symmetry breaking. Ferroelasticity induces polarity by shifting the thermodynamic equilibrium to a non-centrosymmetric space group under uniform strain, provided that such a space group is possible for the material,^[32] while flexoelectricity induces polarity in any centrosymmetric

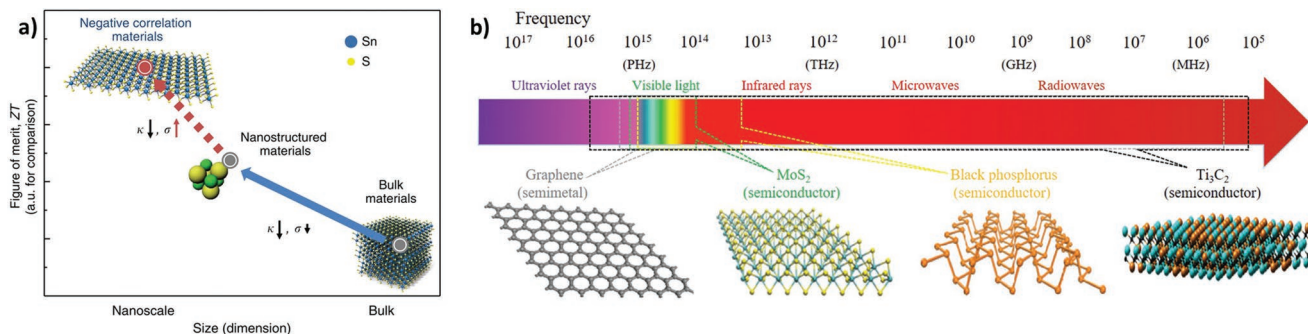


Figure 1. a) Comparison of 2D crystals for energy harvesting from thermal energy, showing increased efficiency going from a bulk powder to a 2D crystal and b) the different optical absorbance and energy harvesting of different classes of 2D crystals. a) Reproduced under the terms of the CC-BY Creative Commons Attribution 4.0 International license (<https://creativecommons.org/licenses/by/4.0>).^[29] Copyright 2016, The Authors, published by Springer Nature. b) Reproduced under the terms of the CC-BY Creative Commons Attribution 4.0 International license (<https://creativecommons.org/licenses/by/4.0>).^[30] Copyright 2020, The Authors, published by Wiley-VCH.

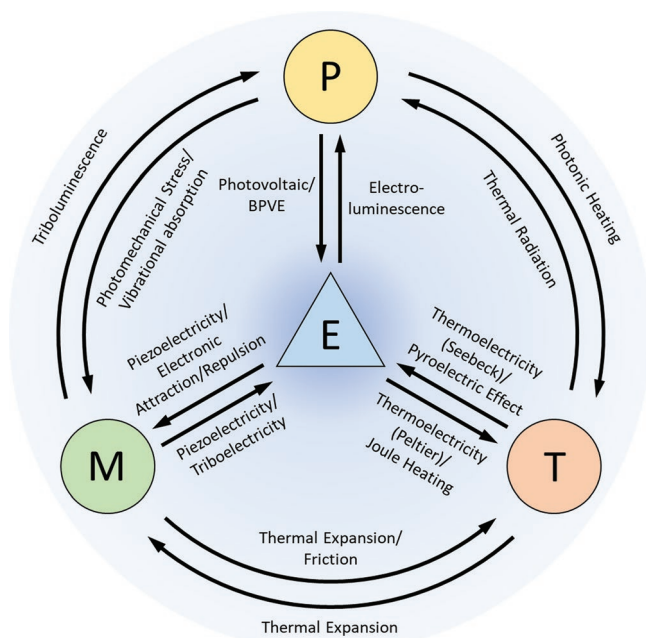


Figure 2. Major forms of energy and the conversion mechanisms between them. These conversion mechanisms can occur simultaneously or concurrently in the same material. *P* = photonic energy, *M* = mechanical energy, *T* = thermal/heat energy, *E* = electrical energy, BPVE = bulk photovoltaic effect. Note these are just the forms of energy-relevant to most energy conversion devices. There are other energy sources that may be exploited, that is, chemical, nuclear, etc.

material by applying an inhomogeneously distributed strain gradient.^[33] Triboelectricity is significantly less well understood,^[34] with triboelectric charge harvesting being attributed to electron tunneling, adsorbed ion transfer, dipole induction, or mechanochemistry (bond cleavage).^[5,35–37] Regardless, it is the build-up of electric charge that occurs during the contact, and motion, between two materials at the interface.

We have recently discussed strategies to enhance *M* → *E* energy harvesting via the piezoelectric effect in 2D crystals.^[17] These strategies included building 2D crystal heterostructures,^[25] strain engineering,^[38] doping through liquid metal synthesis,^[39] and defect engineering to break symmetry in centrosymmetric 2D crystals.^[17] These approaches typically work best with multi-atom 2D crystals such as transition metal dichalcogenides and MXenes.

In contrast, the triboelectric effect can occur in monoatomic 2D crystal structures such as graphene, which can form both the active layer and the electrode.^[40] For example, in contact-separation experiments between two graphene–polymer electrodes, the triboelectric charge was found to depend on the thickness of the graphene layer.^[40] It was shown that the current increased from 100 nA cm^{−2} in bilayer graphene to 250 nA cm^{−2} in monolayer graphene electrodes.^[40] This change was attributed to layer-dependent work function changes in the graphene crystal. The fundamental mechanism that causes the observed charge in the triboelectric effect is still under debate, particularly for resistive, polymeric, and nanoconfined materials.^[5,35] It is currently hypothesized that, given the spatial confinement in 2D

crystals, the observed charge occurs due to electron tunneling phenomena.^[41]

In the context of SMEC with piezoelectricity and triboelectricity—for any piezoelectric material reported in the literature, it is expected there will be a contribution from the triboelectric charge in the current measurements. This comingling of *M* → *E* energy conversion has recently been highlighted by both Sutka et al.^[42] and Chen et al.^[43] Therefore, we employ the general term, mechanical-to-electrical (*M* → *E*) energy conversion, rather than attempt to deconvolute these effects.

3.2. Photo–Electrical (*P* → *E*) Energy Conversion in 2D Crystals

3.2.1. Conventional Photovoltaic Effect

The conventional photovoltaic effect is a photo–electrical (*P* → *E*) energy conversion mechanism that occurs in semiconductors when a photon, with energy greater or equal to the bandgap ($h\nu > E_g$), is absorbed by a valence band (or HOMO) electron and excited to the conduction band (or LUMO) resulting in an electron/hole pair (exciton). To use the electrical energy, the excited charge carriers must be effectively separated by a material interface (most often p–n junctions between electron-favoring (n-type) and hole-favoring (p-type) materials) and then diffuse to electrodes (photovoltaics) or remain at the material surface (photocatalysis) (Figure 3a). Layered 2D crystals exploiting the photovoltaic effect^[44] are emerging as excellent candidates for both solar cells, and as photodetectors down to the near-infrared region.^[45]

Photovoltaic *P* → *E* energy conversion can be enhanced in 2D semiconductor crystals compared to bulk semiconductors due to their unique properties. First, 2D crystals can easily form material junctions by layering 2D crystals on bulk materials or by layering different 2D crystals. The weak vdWs interlayer interactions of the 2D crystals increase the range of materials that can form effective junctions because they minimize the detrimental effects of lattice mismatch, allowing a vast range of band structures that can be optimized for efficient *P* → *E* conversion. Second, 2D semiconductor crystals have a particular advantage over bulk semiconductors in that their nanometer-scale thickness provides the shortest diffusion path possible to the surface or electrode resulting in minimized recombination and excellent photocurrent. Finally, the nanometer-scale thickness of 2D crystals with few or single layers results in very high optical transparency while maintaining functionality. Normally for bulk materials, this reduction in thickness often reduces the total light absorption, which is detrimental for *P* → *E* energy conversion devices. However, some 2D crystals, due to the confined dimensions and momentum states, have van Hove singularities that increase the density of states at the edges of the bandgap, resulting in increased absorption of photons at, or closely above, the bandgap energy.^[46–48] While the photovoltaic effect is the most common *P* → *E* energy conversion mechanism exploited, 2D crystals in particular may exhibit another novel *P* → *E* mechanism; the underexplored bulk photovoltaic effect (BPVE).

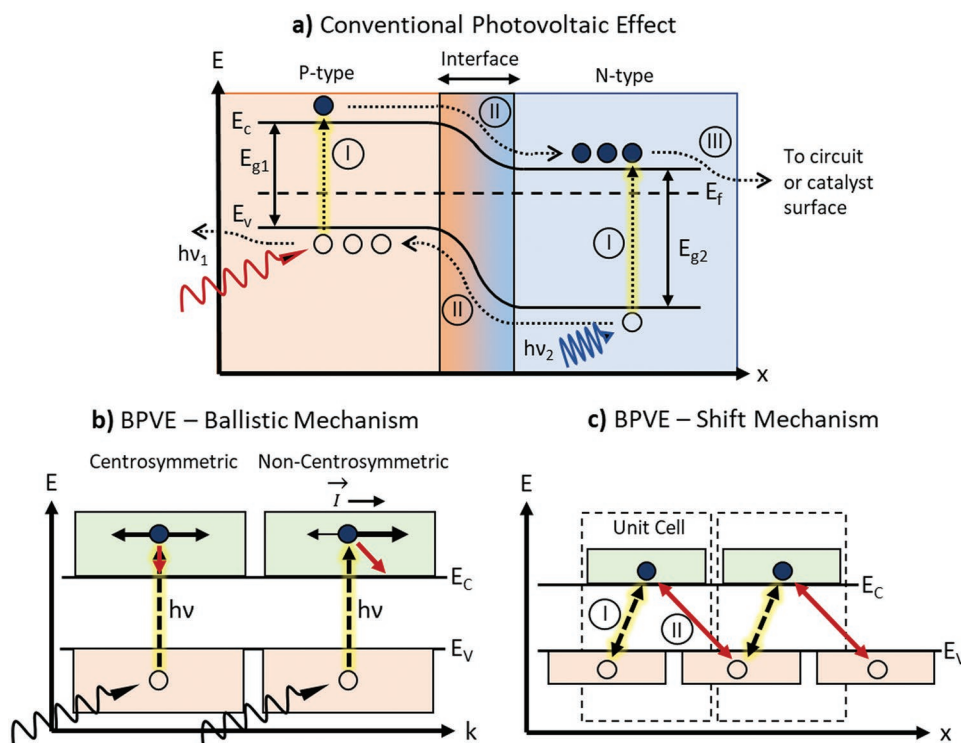


Figure 3. a) Diagram of a conventional photovoltaic device. I) Incident light with energy above the semiconductors' bandgaps will excite an electron from the valence to conduction band. II) A material interface is formed between n-type and p-type semiconductors that have a built-in electric field at the interface, separating charge carriers. III) Separated carriers diffuse to the electrodes or surface. b) Diagram of the ballistic mechanism of the bulk photovoltaic effect (BPVE). Non-centrosymmetric crystals have an asymmetric distribution of hot-carrier momentum, resulting in an averaged movement of carriers in the crystal as the bulk photocurrent. c) Diagram of the shift mechanism of BPVE. I) These are radiative transitions that can occur through absorption or emission of photons. Under light irradiance, photoexcitation from a valence to conduction level in a shifted lattice location often occurs, while some carriers relax through the same transition releasing a photon. II) These are non-radiative transitions that only occur from emitting or absorbing many phonons. The non-radiative transition from a conduction to valence level at a shifted lattice location occurs by release of many phonons through the lattice. However, the non-radiative transition from valence to conduction levels requires an extremely large phonon or thermal fluctuation, or many additive phonons must be absorbed simultaneously, which is extremely unlikely. This results in charge carriers being effectively blocked from backward transitions and thus a shift in current is exhibited.

3.2.2. Bulk Photovoltaic Effect (BPVE)

The BPVE is a $P \rightarrow E$ energy conversion mechanism that only occurs in non-centrosymmetric materials.^[49,50] The mechanism is different from the conventional photovoltaic effect because a material interface, or p–n junction, is not required to generate a photocurrent. Two distinct mechanisms have been proposed for BPVE. The “ballistic” mechanism states that photoexcited, non-thermalized carriers have an asymmetric momentum distribution due to the non-centrosymmetric polarized structure of the crystal, resulting in an overall biased movement of excited carriers (a current) under illumination in the crystal (Figure 3b).^[51] This movement of hot carriers is limited to the ballistic length (mean free path) of the carrier in the crystal, which varies from often a few nm up to 100 nm depending on the crystal. This results in an effective BPVE current only from the crystal region within the free path length from the electrode.^[52] The “shift” mechanism is based on quantum mechanics and proposes that photoexcitation of an electron in the non-centrosymmetric crystal results in a real space shift of the electron by a unit cell/mean free path in the crystal polarization direction (Figure 3c).^[50,53]

However, a shift in the reverse direction requires absorption of a similar amount of only thermal (phonon) energy. A thermal fluctuation that large is very unlikely, so the reverse current is effectively blocked resulting in a net “shift” current from the BPVE. Regardless of the mechanism, the photocurrent from the BPVE is vastly increased when the material thickness is below the electron mean free path.^[54]

It is clear that layered 2D crystals are uniquely positioned to exploit the BPVE effect as they have nanoscale thicknesses usually less than the mean free path, and consequently can deliver a large photocurrent from the BPVE.^[49,54–57] The photovoltages that can be obtained from the BPVE are orders of magnitude higher than the materials' bandgaps that constitute the limit for conventional photovoltaics.^[58,59] This is useful for applications that require higher voltages than typical bandgaps. The $P \rightarrow E$ conversion efficiency with the BPVE can also surpass the theoretical Shockley–Queisser efficiency limit of $\sim 33\%$ for the conventional photovoltaic effect due to the efficient use of hot carriers.^[50,52,55] Thus, BPVE potentially provides a route to extremely efficient and thin $P \rightarrow E$ energy conversion devices.^[52,56]

3.3. Thermo–Electrical ($T \rightarrow E$) Energy Conversion in 2D Crystals

3.3.1. Pyroelectric Effect

The pyroelectric effect is an understudied mechanism for energy conversion in 2D crystals. Like the piezoelectric effect, where dipoles reorient under mechanical stress, in the pyroelectric effect dipoles reorient due to a temperature change. Importantly, current is only generated transiently during temperature changes, not at a constant temperature. The dipole change places pyroelectric materials in the family of dielectric-to-ferroelectric systems. Many 2D crystals have been reported to be pyroelectric.^[60] While the fundamental mechanisms behind pyroelectricity in 2D crystals are still under investigation, the current understanding is that lattice deformation during heating gives rise to spontaneous polarization vector changes that facilitate thermo–electrical ($T \rightarrow E$) energy conversion.^[60] This process is often exploited for photodetector and thermal energy recovery system applications.

Unlike piezoelectricity, which requires asymmetry, pyroelectricity requires unit cells that are polar. For this reason, fewer 2D crystals will exhibit pyroelectricity compared to piezoelectricity. Despite this, there are recent reports of the pyroelectric effect being exhibited by select 2D crystals, notably black phosphorene,^[61] and indium selenide.^[62]

The relative lack of reports of pyroelectric effects in 2D materials is because the pyroelectric effect, in general, is simply less studied than other energy conversion phenomena such as piezoelectricity or thermoelectricity. A simple literature search shows that only 2.5% of the 3.6 million papers reporting piezoelectric, ferroelectric, thermoelectric, and pyroelectric effects relate to pyroelectricity. This presents a major opportunity for research into novel layered 2D crystals exhibiting the pyroelectric effect in the future, particularly for catalytic applications.^[13]

3.3.2. Thermoelectric Effect

In contrast to the pyroelectric effect, that generates charge during changes in temperature for the entire material, the thermoelectric effect generates charge from a temperature gradient across the material. Thus, $T \rightarrow E$ energy conversion from the thermoelectric effect is constant when the temperature gradient is constant. The thermoelectric effect is proportional to the electrical conductivity and inversely proportional to the thermal conductivity of the material. Importantly, in the context of 2D semiconducting crystals, the Seebeck coefficient (that defines the thermoelectric output) is proportional to the energy derivative of the electronic density of states at the Fermi level.^[63,64] Therefore, effects that alter these states, such as photoexcitation, strain, or doping, will alter the corresponding thermoelectric outputs (Section 4). The thermoelectric effect, and devices such as thermoelectrochemical cells,^[65] are emerging as key tools for wearable energy harvesting devices, providing supplemental power to energy storage systems.^[66]

2D crystals have recently been found to possess extremely high thermoelectric figures of merit (ZT), in particular, 2D tin selenide (SnSe) crystals (ZT \approx 2.62 at 923 K)^[67] and defect-engineered 2D SnSe (ZT \approx 2.4 at 800 K) crystals.^[68] The reason

for the high ZT in 2D crystals is likely due to the anharmonic bonding and poor interlayer interactions that result in very low thermal conductivity.^[67] Stacked 2D crystal heterostructures can exhibit much lower out-of-plane thermal conductivity due to vibrational mismatch and increased interlayer spacing,^[69] and thus can have higher ZT. Novel unexplored 2D tetragonal pnictogen (P, As, Sb, or Bi) crystals have also been predicted by combined density functional theory and machine learning (ML) analysis to have very high thermoelectric constants (ZT \approx 3.22 for 2D tetragonal Sb) with high thermoelectric conversion efficiency due to their very low lattice thermal conductivity.^[70]

4. Energy Interplay in Materials

The different types of energy conversion mechanisms in a material are most often not independent of each other; they are interconnected, and multiple conversion mechanisms can occur simultaneously or consecutively. Energy converted within the material can apply a new force or can change a material state that can impact the magnitude and efficiency of the other energy conversion mechanisms. External forces like material stress, or electric fields applied to the material, can amplify or inhibit energy conversion mechanisms. In addition to forces applied internally and externally, the energy interplay may cause positive feedback from additive effects that enhances the efficiency of energy conversion, or the energy interplay may cause subtractive effects or convert to non-useful energy (e.g., heat), consequently decreasing energy conversion efficiency in the materials. All interconnected mechanisms must be considered when investigating, designing, and characterizing new energy conversion materials for applications. Section 4 demonstrates some internal or external forces that can impact other energy conversion mechanisms and discusses energy interplay effects in materials.

4.1. Effect of Mechanical Stress on Energy Conversion Mechanisms

4.1.1. Constant Mechanical Stress for Optimizing Photo–Electrical Conversion

Applying stress to semiconductors to strain and deform their crystal lattice changes their electronic band structure by varying the lattice constants and the electron density distribution.^[71] Lattice deformation can vary the size of the bandgap^[72] and/or change it from an indirect to a direct bandgap, thereby affecting $P \rightarrow E$ conversion mechanisms (Figure 4).^[73] Additionally, stress can be applied intentionally to optimally tune the band structure for different applications (strain engineering). For $P \rightarrow E$ conversion, stress is often applied to tune the band structure of the material to achieve bandgaps that absorb more of the solar spectrum.

Layered 2D crystals can handle much higher strain deformation before rupture (25% lateral strain for monolayer graphene,^[74] 11% lateral strain for MoS₂)^[75] than conventional bulk semiconductors, so are ideal materials for strain engineering.

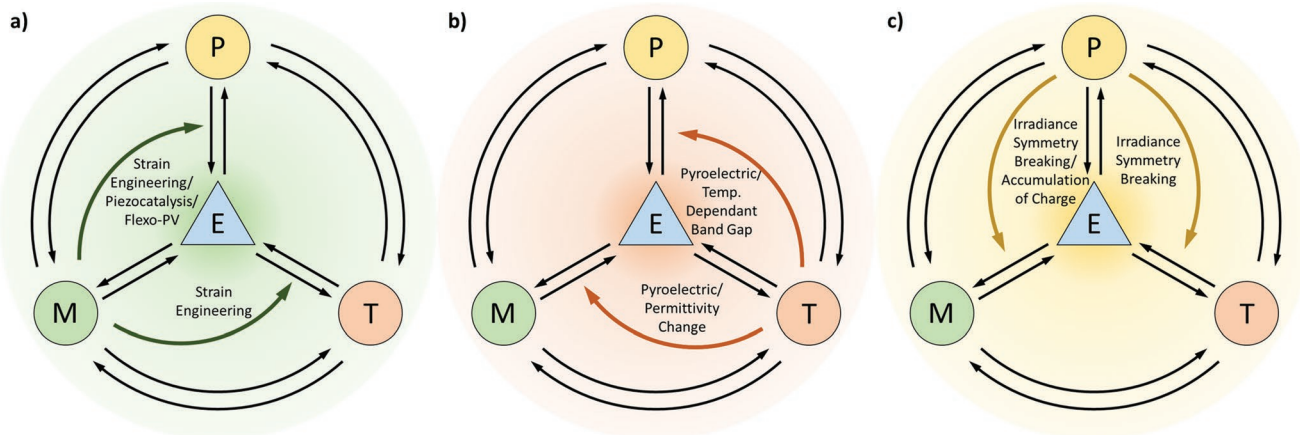


Figure 4. a) Effect of mechanical stress on photo–electrical and thermo–electrical conversion mechanisms. b) Effect of temperature and temperature change on photo–electrical and electro–mechanical conversion mechanisms. c) Effect of light irradiance on thermo–electrical and electro–mechanical conversion mechanisms.

Stacked multilayer 2D crystals can have in-plane strain-induced differently to each layer resulting in unique band structures. Also, the out-of-plane strain induced in stacked multilayer 2D crystals can affect the interlayer exciton binding energy.^[76] The strain in stacked 2D crystals can also change the ratio of photoluminescent emission intensity between the stacked layers, with compressive and tensile strain inversely proportional to the intensity ratio.^[77]

Lateral strain can be induced by lattice mismatch between the 2D crystal and the substrate/other layers by using flexible substrates and bending/straining the substrate, or by using patterned substrates with corrugated/bumpy features.^[78] Wrinkling or folding 2D semiconductor crystals can induce local strain in the bent region of the material, varying the bandgap and photon absorption/emission in a chemically homogenous material.^[78,79] This can enable broad-spectrum absorption of light frequencies with a single material device, maximizing absorption of the solar spectrum and increasing $P \rightarrow E$ energy conversion from solar cell devices.^[80]

The application of non-uniform stress, either from extrinsic sources (e.g., bending of a flexible substrate) or intrinsic sources such as non-coherent (or twisted) stacking of layers, can induce a strain gradient and consequently break symmetry in centrosymmetric materials, termed flexoelectricity. The latter case is particularly interesting as it employs intermolecular forces to deform the unit cell of the layer at the local scale.^[81] In addition to altering the band structure, flexoelectric strain gradients can act to enhance the $P \rightarrow E$ energy conversion through the introduction of a shift current, caused by spatial electron displacement and the resultant photon-induced interband excitation from the valence band into the conduction band.^[82] This shift current forms part of the BPVE in non-centrosymmetric materials.^[83] The BPVE is unique, capable of exhibiting a generated photovoltage greater than the bandgap of the material (that is, exceeding the Shockley–Queisser limit); however, the drawback of this effect in conventional non-centrosymmetric materials (e.g., ferroelectrics and piezoelectrics) is the often low $P \rightarrow E$ energy conversion.^[52] The flexo-photovoltaic effect^[84] in 2D materials could provide a pathway to overcome this

limitation, with reports demonstrating short circuit currents that are orders of magnitude greater in comparison to bulk ferroelectric materials.^[82,83] This improvement was attributed to the semiconducting nature of such 2D crystals and reduced dimensionality.^[85,86] The synergy between flexoelectricity and BPVE is promising to further tailor the bandgap in semiconducting 2D crystals.^[55]

4.1.2. Dynamic Mechanical Stress for Optimizing Photo–Electrical Conversion

The complexity of interaction increases dramatically when multiple simultaneous inputs are applied to a material surface. For example, the WSe_2 or MoS_2/WS_2 heterostructures for photoelectrocatalytic water oxidation,^[87–90] are represented in **Figure 5** as the generic formula MX_2 . Here, a visible-light photon is absorbed by the semiconducting 2D crystal (Figure 5a,b), generating an exciton whereby h^+ reacts with water to produce oxygen and the e^- is withdrawn (Figure 5c). However, the continuous reaction leads by design to the evolution of gas bubbles (or at least a pressure change) on the 2D crystal electrode (Figure 5d, top). Both pressure changes from this gas bubble evolution, and water filling the void produced by the bubbles leads to significant induced stresses on the electrode, proportional to the amount of water oxidation occurring. How these stresses dynamically alter the electronic band structure of such 2D crystals (Figure 5d,e) is not well studied, but could be critical for understanding the rate limitations and chemical stability of these systems over time. For example, the bandgap of a WSe_2 monolayer is approximately 1.7 eV,^[91] and a WSe_2 -based heterostructure with just 4% tensile strain has produced 1.37 V via the piezoelectric effect.^[92] This means that even very small strains induced by pressure fluctuations in situ will result in significant temporal band structure modulation.

Such effects can further be modulated when 2D semiconducting crystals are decorated with catalytically active nanoparticles, as is often described by Sivula et al. in state-of-the-art

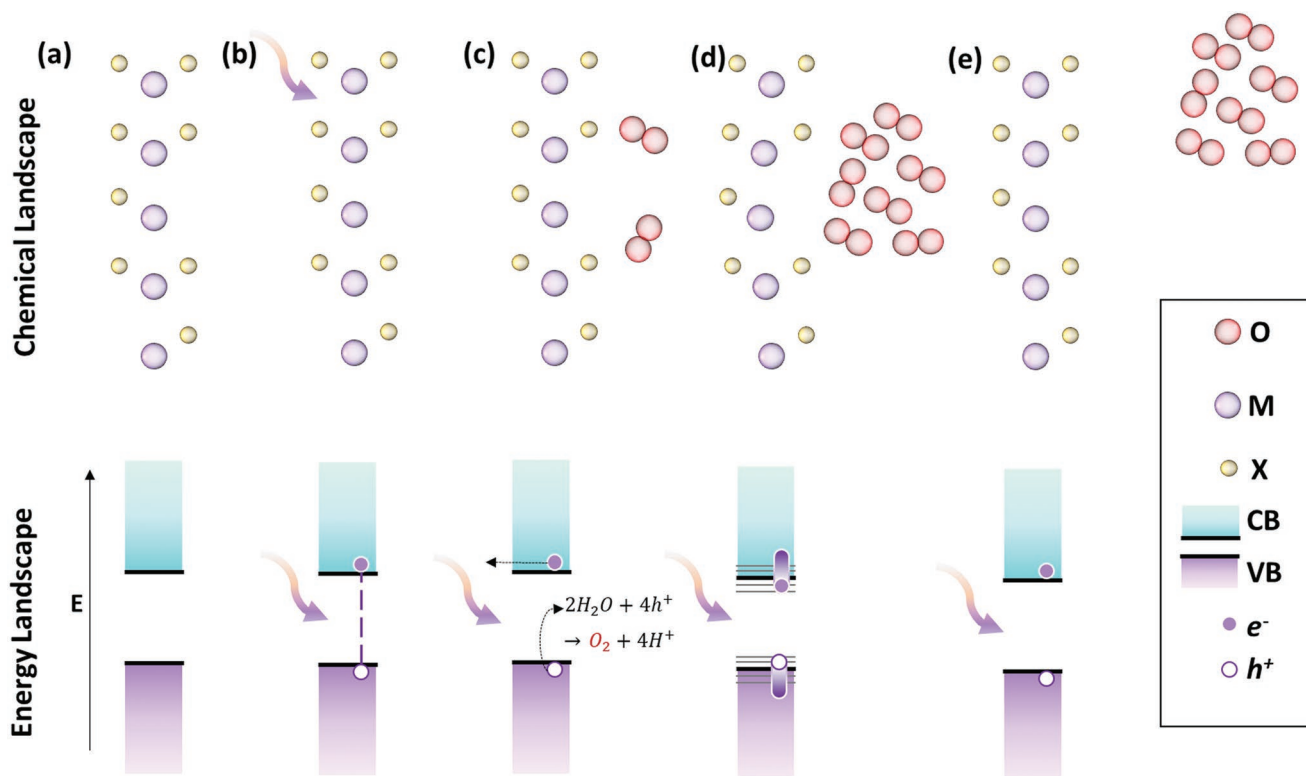


Figure 5. Schematic of alteration of the electronic band structure of a 2D crystal (MX_2) during the oxygen evolution reaction due to mechanical force. a) The initial electronic state of the 2D crystal; b) a visible-light phonon interacts with the 2D crystal, generating an exciton (electron-hole, e^-h^+ pair); c) h^+ reacts with water at the interface forming oxygen molecules, the e^- is removed for the opposing half-reaction. d) The continued evolution of oxygen molecules leads to a pressure change at the reaction site, with a subsequent deformation of the 2D crystal lattice. If the 2D crystal is piezoelectric this deformation will result in a change in the electronic structure, changing the effective optical bandgap, and band edge alignment; and e) the cluster of oxygen species (including radicals and O_2 molecules) disperses away from the active site, restoring the original lattice configuration and electronic structure (noting that during the relaxation of the structure the effective bandgaps and edges will be shifted in an opposite way to in (d)). In the legend, O = oxygen, M = metal; X = chalcogen; CB = conduction band, VB = valence band; e^- = electron; and h^+ = holes.

water oxidation experiments.^[89,90,93] In another example, the strain induced by catalytically active gold nanoparticles on an MX_2 lattice has been investigated by Singh et al.^[94] They showed that there was between 9% and 10% biaxial compressive strain induced in a MoS_2 monolayer due to electron injection from physisorbed gold nanoparticles.^[94] Whilst this strain is significant, it is even more critical to note that 50 nm away from the gold nanoparticle, the lattice was unstrained, meaning the electronic structure of the 2D crystal was highly heterogeneous under these conditions, causing photon absorbance to vary greatly.

The concept of stress generation by bubbles for enhanced catalysis has also been studied in the context of the piezoelectric effect by Bößl and Tudela.^[95] In their proposed system, externally applied ultrasonic waves generate regions of high and low pressure within the fluid. These varied pressure regions lead to vapor bubble formation via cavitation. The bubbles then undergo a process called asymmetric bubble collapse^[96] on the surface of a catalyst, which induces stress on the catalysts, thus activating the piezo-catalytic system.^[95] While the majority of reports on PC systems focus on traditional piezoelectric (non-2D) crystals, there are recent reports of PC in transition metal dichalcogenides,^[97,98] monochalcogenides,^[99] oxides,^[14,99] and phosphides.^[99,100]

It is likely that as engineering out-of-plane piezoelectricity in 2D crystals is realized,^[17] 2D crystals will emerge as the most popular PC materials. This is due to their inherently catalytic activity for key reactions of interest^[101] and the relative flexibility of 2D crystals enabling greater deformations via bubble cavitation and collapse, subsequently generating significantly more catalytic enhancement compared to traditional, non-2D piezoelectric crystals.^[102]

Here, it is important to distinguish the two phenomena discussed in the previous paragraphs: in situ bubble formation due to catalytic processes; and externally stimulated bubble formation via ultrasonic waves. In the first system, these effects may have already been observed in the catalysis literature, albeit not discussed nor understood. However, in the second system, where cavitation is being specifically exploited, it is critical to understand whether this energy interplay is providing any net benefit to the catalytic system. A simple way to assess this efficiency is to measure the average property change under the stimulation conditions. For electrocatalysis, this can be achieved by comparing the voltage needed for the reaction to occur with the theoretical E_0 of the reaction.

$$\eta = \frac{(E_0 \times I) - P_i}{E_{\text{cell}} \times I} \quad (1)$$

where η = efficiency; E_0 is the reaction potential of a given reaction; I is the measured current; P_i is the input power to enhance the catalyst; and E_{cell} is the measured potential.

Thus, if the improvement in measured current or potential is less than the total power input into the system these stimulation mechanisms will not provide a net energy benefit. However, they may play a useful role in the remote activation of electronics embedded in the environment or the human body.

4.2. Effect of Heat/Thermal Effects on Energy Conversion Mechanisms

The relationship between thermal energy/temperature with photonic, mechanical, and electrical energy conversion mechanisms is well known (Figure 4b). Indeed, the importance of temperature in energy transfer is so well understood that it is controlled as a standard in all chemical reactions to ensure reproducible results.

However, in terms of interaction with other energy conversion mechanisms, thermal energy has traditionally been considered a separate class of energy, and the almost ubiquitous control of temperature in experiments has led to few opportunities to study the interplay of these effects. Thermal energy is particularly impactful when coupled to $P \rightarrow E$ energy conversion and electrochemical energy storage. For example, by mounting a typical thermoelectric 2D crystal on a heat sink, the thermal energy incident from the sun naturally generates a temperature gradient that can modulate the band structure of the 2D crystal and enhance light energy harvesting ($P \rightarrow E$ energy conversion) (Figure 4b). In fully integrated photoelectrochemical (PEC) cells, excess thermal energy in the photovoltaic component can be exploited for improving the catalyst kinetics in the electrolyzer component and thus increasing catalytic, electrochemical energy conversion efficiency.^[103] In contrast to the beneficial effect in PEC cells, heating triboelectric ($M \rightarrow E$) generators have been shown to decrease $M \rightarrow E$ conversion.^[104,105] This was attributed to changes in the permittivity of the sample during heating, leading to less available charge storage on the surface of the triboelectric generator.^[104]

4.3. Effect of Light Irradiance on Energy Conversion Mechanisms

In contrast to enhancement of energy absorption effects, constant light irradiance on some materials can break crystal symmetry or couple with energy conversion processes to enhance non-photo conversion mechanisms. It has recently been shown that photon absorbance can transiently break unit cell symmetry for the Weyl semimetal tantalum arsenide (TaAs) due to changes in electronic polarization from photocurrent generation.^[106] The effect is purely electronic; no structure/lattice changes occur. This effect means that TaAs under light irradiation will exhibit piezoelectric and pyroelectric effects (Figure 4c). Many other materials may exhibit this effect, in particular, Weyl semimetals and transition metal mononpnictide.

Recently, Chen et al.^[107] have reported a dramatically enhanced electrical output from triboelectric poly(dimethylsiloxane) (PDMS) by coupling to photon absorption in illuminated 2D

graphitic carbon nitride (g-C₃N₄)/2D MXenes/Au clusters dispersed in the PDMS film. The proposed cause of the boost in performance was that the photovoltaic effect, occurring under light irradiance on the g-C₃N₄/MXene/Au clusters, causes an accumulation of trapped charges around the clusters in the triboelectric film. The increased accumulated charges add to the charge flow during the triboelectric effect and increase the total triboelectric power output. This demonstrates the effect of coupling of light irradiance charge flows on other energy conversion mechanisms.

4.4. Thermo-Photo-Mechanical-Electrical Conversion and Energy Interplay

Past research in particular energy conversion mechanisms has clearly identified energy interplay effects. However, proper characterization and analysis of the entire network of dynamic energy conversion mechanisms occurring simultaneously or concurrently in materials during apparently simple energy conversion processes is critical but rarely performed. Research often focuses on the efficiency and process of the main energy conversion mechanism of interest in the material. Furthermore, with the addition of more simultaneous energy inputs to the material, simplistic models of additive or subtractive coupling between input energies fail to convey the complexity of the rich interplay of energy conversion mechanisms.

For instance, conventional photovoltaic devices are well researched, but the $P \rightarrow E$ energy conversion is often reported in isolation from any quantitative analysis of the energy interplay that occurs during their operation. Figure 6 shows the energy interplay network for photovoltaic devices where $P \rightarrow E$ conversion (photovoltaic) in the material can occur

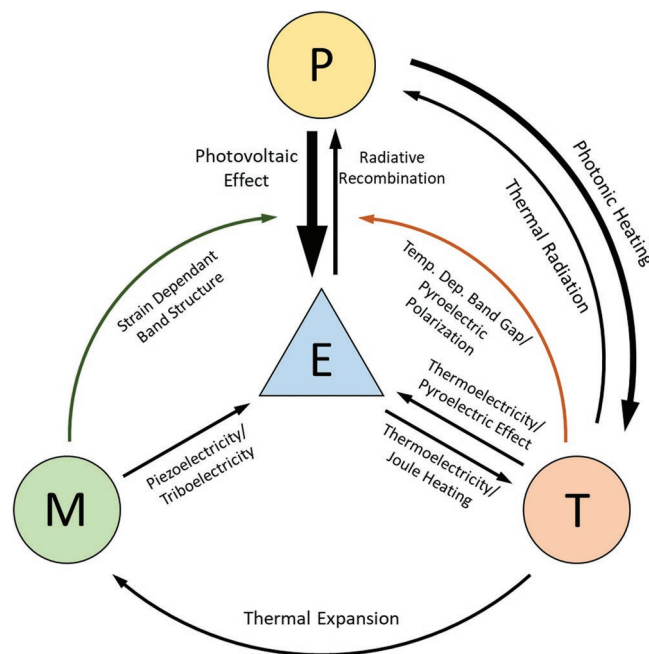


Figure 6. The energy interplay network for conventional photovoltaics.

simultaneously with $P \rightarrow T$ conversion under incident light. However, the extra thermal energy generated can thermally expand the material causing material strain; and/or, the localized thermal energy can cause a temperature gradient and result in dipole polarization due to the pyroelectric effect. The material strain or polarization will impact the electronic structure of the material and thus impact the $P \rightarrow E$ conversion. Additionally, heating can lead to mechanical vibration and friction at interfaces (due to differences in coefficients of thermal expansion), which can lead to $M \rightarrow E$ (triboelectric) energy conversion. To truly understand energy conversion processes critical to applications like energy harvesting, optoelectronics, and others, the entire energy interplay network of a material must be characterized and analyzed.

Some research has explored the exploitation of this rich energy interplay in material composites or multicomponent devices for extended or enhanced functionalities. Jia et al.^[108] demonstrated a flexible e-skin device that emits light when it was touched, by incorporating a ZnS:Cu-embedded polyvinylidene fluoride-co-hexafluoropropylene (ZEPH) composite film that exhibited triboelectricity ($M \rightarrow E$) to provide energy for photoluminescence ($E \rightarrow P$). However, only the output light spectrum and intensity were measured, along with the applied mechanical force. The electrical energy generation and conversion were not characterized; however, the authors modeled some of this energy interplay in the composite. Cheng et al.^[109] reported an Ag/SiO₂ hybrid nanostructure for highly efficient (99% over solar range) $P \rightarrow T$ energy conversion, which was coupled to a thermoelectric material to convert that thermal energy to electrical energy, making an efficient $P \rightarrow T \rightarrow E$ energy conversion solar light-harvesting device. The energy interplay was characterized by first measuring the temperature increase of the material from light irradiance, and then measuring voltage output when coupled to a thermoelectric device, although heat generation and conversion through the thermoelectric device were not directly monitored. Yang et al.^[110] demonstrated a multicomponent device that integrated a piezoelectric/pyroelectric polarized polyvinylidene fluoride (PVDF) film with an aligned ZnO nanowire array/poly(3-hexylthiophene) (P3HT) heterojunction solar cell to simultaneously harvest mechanical, thermal, and light energy as a SMEC device. The energy conversion mechanisms exploited from each component were characterized separately, the total voltage output was measured, and the energy interplay during SMEC was noted; however, the energy interplay was not quantitatively measured or modeled. Photovoltaic/thermal (PV/T) systems are amongst the most intensely investigated multicomponent energy interplay devices. PV/T systems have thermal energy harvesting components attached to photovoltaic cells to synchronously harvest the thermal energy generated during solar light irradiation, thus increasing the total amount of usable energy harvested from sunlight.^[111] However, limited research has been conducted on exploiting energy interplay in single materials, important for energy harvesting technology, and thus there is scarce research on SMEC materials. Regardless, some SMEC materials have been theoretically proposed to exist, specifically layered 2D crystal vdWs heterostructures.^[112]

5. Promising SMEC Materials—Ferroelectric 2D Crystals

Ferroelectric 2D crystals are promising candidates for SMEC materials.^[113,114] Ferroelectric materials can simultaneously harvest energy from the major environmental energy sources of heat, mechanical energy, and light. Ferroelectric materials have non-centrosymmetric crystal structures and permanent dipoles that allow them to operate as piezoelectric and pyroelectric materials and demonstrate $M \rightarrow E$ and $T \rightarrow E$ energy conversion, respectively (Figure 7). Importantly, ferroelectric crystals exhibit the BPVE (Section 3.2.2) for $P \rightarrow E$ energy conversion, where they can generate larger BPVE photocurrents than non-ferroelectric non-centrosymmetric crystals due to better carrier management^[52] and photocurrent stimulation from non-polarized light.^[49] BPVE photocurrents are also drastically increased in ferroelectric 2D crystals due to their nanoscale thickness which is shorter than the electron mean free path.^[55] Typical ceramic bulk ferroelectrics have BPVE photocurrents that are too low to be useful for energy harvesting, therefore using ferroelectric 2D crystals is necessary to achieve reasonable BPVE photocurrents for devices. Additionally, ferroelectric materials can, under certain conditions (e.g., in layered crystals with 2D flakes), act as excellent thermoelectric materials as an additional $T \rightarrow E$ energy conversion mechanism.^[115–117] Layered 2D crystals have severely reduced out-of-plane thermal transport due to reduced interlayer interactions, which can greatly increase thermoelectric energy conversion. All together these properties make ferroelectric 2D crystals promising SMEC materials and thus should be further investigated. Layered 2D crystals further possess mechanical flexibility, high mechanical strength, durability, and thin-film formability, which makes them ideal SMEC materials for small-scale and personal energy harvesting devices. SMEC 2D crystals could also be used as advanced electrocatalysts that are enhanced by multiple energy sources and high surface area-increased kinetics.^[118]

An example of potential ferroelectric 2D crystals with multiple energy conversion mechanisms is described in a recent report on 2D copper indium thiophosphate, CuInP₂S₆ (CIPS), crystals.^[55] These crystals exhibited an enhanced BPVE effect

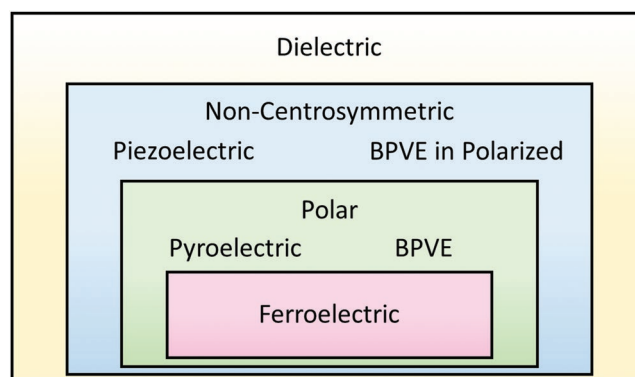


Figure 7. The hierarchy of dielectric-to-ferroelectric materials, whereby all pyroelectric materials are piezoelectric but not all piezoelectric materials are pyroelectric, and all ferroelectric materials are both pyroelectric and piezoelectric.

that was two orders of magnitude higher than typical bulk ferroelectric perovskite oxides due to the nanoscale thickness of the material being smaller than the electron mean free path.^[55] The best cell had $\approx 3\%$ reported efficiency with irradiance from a 405 nm laser, despite only having $\approx 3\%$ absorbance at that wavelength. 2D CIPS crystals have also been reported to have a very large d_{33} out-of-plane piezoelectric coefficient of -95 pm V^{-1} at 10 kHz,^[119] and generate reasonable current from the pyroelectric effect operating around room temperature ranges.^[120,121] Additionally, Weyl semimetal TaAs has been shown by Osterhoudt et al.^[122] to have very large BPVE photocurrents under mid-infrared light irradiance, which would be very useful for infrared solar cells. The subset of stable ferroelectric 2D crystals is likely to be quite limited due to the general instability of ferroelectricity with reduced material dimension/thickness.^[113,123,124] However, recent work has presented some stable room temperature ferroelectric 2D crystals including MoTe_2 ,^[125] the family of $\text{III}_2\text{-VI}_3$ 2D crystals like In_2Se_3 ,^[124] 2D CIPS crystals, and TaAs as mentioned earlier,^[55,122,126,127] and many others.^[113,128–130] Ferroelectricity may arise in a specific number of layers of 2D crystals that have non-ferroelectric monolayers, like bilayer or trilayer WTe_2 ,^[131] or multilayer SnTe .^[129] Ferroelectricity may also be engineered in 2D crystals by structural modifications, or through 2D crystal hybrid structures. Such ferroelectricity-inducing modifications include construction of vdW heterostructures (stacked 2D crystals layers of different types),^[112,132] elemental substitution on one side of a 2D crystal layer to synthesize Janus 2D crystals,^[133] or even fabrication of moiré-patterned ferroelectric domains in twisted bilayers of non-ferroelectric 2D crystals.^[132,134] The range of possible ferroelectric 2D crystal structures can therefore be extended with engineered materials and novel device structures, presenting an opportunity for material scientists and device engineers to discover powerful and efficient SMEC materials for advanced multiple energy sources harvesting applications.

6. Outlook

There is little doubt that 2D crystals provide an exceptional template to harvest mechanical, thermal, or photoenergy and will play an important role in new engineering systems where simultaneous harvesting of two or more of these energy inputs will transform ambient energy harvesting for society. The following summarizes the outlook of understanding and rationalizing the effects that energy interplay will have on energy harvesting materials and the search for idealized SMEC materials.

6.1. Understanding Energy Interplay Materials

Ingenuously designed materials can potentially take advantage of energy interplay to harvest useful energy from multiple environmental energy sources or to amplify an energy conversion mechanism to increase conversion efficiency. To clarify the role of different materials and their energy interplay in energy harvesting research, we propose four types of useful

Table 2. Proposed energy conversion material types.

Type	Energy conversion mechanism	Energy input(s)	Energy interplay
Type 1	Synchronous multisource (SMEC+)	Multiple	Additive
Type 2	Synchronous multisource (SMEC-)	Multiple	Subtractive
Type 3	Internally amplified	Single	Additive
Type 4	Externally amplified	Single	Additive

energy interplay materials for fabricating advanced energy conversion devices (Table 2). Type 1 and 2 energy interplay materials can harvest useful energy from multiple energy sources. Type 1 (SMEC+) materials have additive interplay effects where multiple energy sources complement or overlap each other, resulting in SMEC with greater or equal energy conversion compared to the sum of each single-source energy conversion. In contrast, Type 2 (SMEC-) materials have subtractive interplay effects where SMEC results in lower energy conversion than the sum of each single-source energy conversion. Types 3 and 4 energy interplay materials can harvest useful energy from single energy sources. Type 3 materials have energy interplay that can internally amplify the effectiveness/efficiency of the energy conversion process via additive interplay effects. Type 4 materials utilize additive applied energies/forces to externally amplify the conversion efficiency (e.g., strain engineering).

2D crystals, due to their efficient energy conversion mechanisms and extremely wide range of structures and properties, are a prime class of materials for SMEC materials. Energy interplay may be obtained with multi-component systems, however, single materials will have a greater potential for scale-up, utility, and wider applications due to their simplicity and reduced component volume.

6.2. Effects of Energy Interplay on Characterizing Energy Harvesting Materials

The complexity of energy interactions in multisource energy harvesting has been known for over half a century.^[135,136] Designing 2D crystals to exploit these complementary energy conversion phenomena will herald a new era of ambient energy harvesting. However, it should be remembered that SMEC phenomena is likely to have been present in published studies but is almost always not reported as such, so expectations for rapid advances should be tempered. A critical reassessment of measurement techniques for mechanical, electrical, and light-based energy harvesting is required. Researchers must acknowledge that reported data for energy conversion from a single energy source are fundamentally entangled with conversion from other energy sources, as described by Lang in 1974, and entangled with the interplay from other energy conversion mechanisms. A summary of the common effects discussed, and their overlap is provided in Figure 8.

Furthermore, terminology must be used more accurately and consistently. For example, in many cases, it may be more accurate to report the total measured $M \rightarrow E$ energy conversion, particularly where triboelectric, piezoelectric, and/or flexoelectric contributions have not been deconvoluted. More broadly, in $T \rightarrow E$ and $P \rightarrow E$, the effects of $M \rightarrow E$ conversion are likely

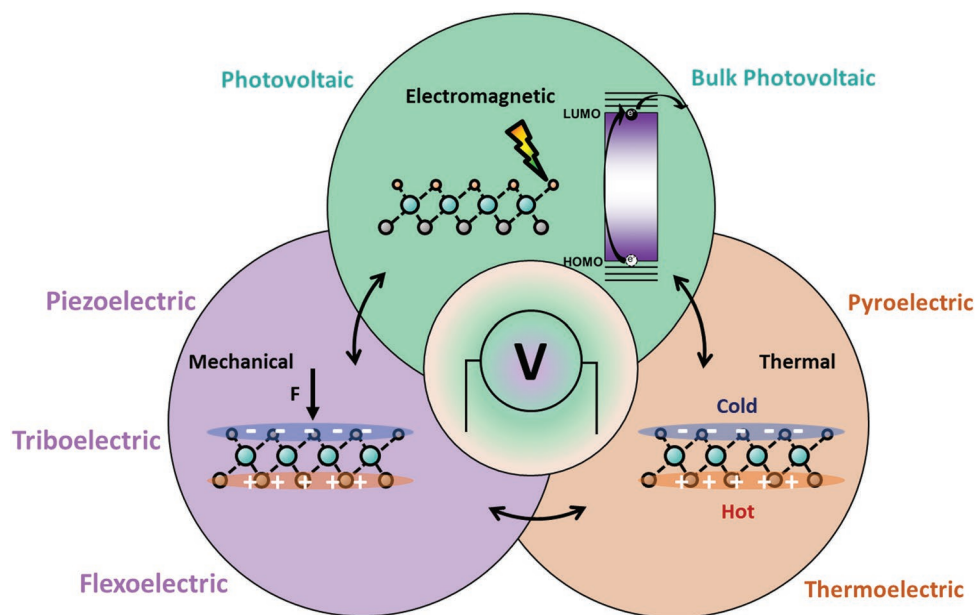


Figure 8. Energy harvesting from mechanical, electromagnetic, and thermal sources from a layered 2D crystal, highlighting the array of complementary and competing effects.

less as they are typically more static systems, but it is worth considering the role that SMEC can have in enhancing or affecting measurements. The clearest case to consider these effects is in wearable style energy harvesting and sensing devices that experience friction, deformation, light irradiation, and a temperature gradient simultaneously.

For larger-scale energy harvesting devices, where thermal gradients and optical transparency can vary, reporting the total energy output or ambient-to-electrical energy conversion is far more representative of the processes occurring. This ignores the “elephant in the room”; parasitic charge loss from poor electrical connections and circuitry that is often ignored in the characterization of energy harvesting materials and devices making accurate quantification of energy conversion in materials challenging.

6.3. Applications of SMEC Materials & Devices

The key advantages of SMEC materials are twofold; a significantly higher charge and energy output compared to single-input energy harvesters; and a combination of fast charge spikes (i.e., from mechanical deformation) and continuous charge generation processes (thermoelectric, photovoltaic). These key advantages should accelerate the future applications of SMEC materials in a wide range of application areas. These applications fall broadly into three classes; 1) energy harvesting; 2) green chemistry; and 3) quantum data storage.

6.3.1. Energy Harvesting

SMEC materials in energy harvesting devices can capture energy from the environment which would otherwise dissipate

as loss mechanisms. This makes them optimal for energy harvesting devices used to power small-scale, mobile, remote, and personal/body-mounted devices. Maximizing the ambient energy harvested by utilizing multiple energy sources is critical to ensure the effective powering of these devices. SMEC materials can be used to power wearable electronics, allowing them to be powered by the movement of the body, by sunlight on the wearable device, and by body heat and solar heat concurrently. SMEC materials can be further coupled to sensors and devices on industrial equipment, engines, and motors, allowing them to be powered by engine heat and vibrations. For these systems, the magnitude of total energy captured is critical for minimizing weight, footprint, and lifetime of the device, and thus SMEC materials provide a clear advantage. In addition, the different timescales of thermal, mechanical, and photo charge generation allow SMEC materials to function as a multi-input self-powered monitoring device, whereby signal from different sources can be collected and deconvoluted in a single system. Effective self-powering and multi-input sensing can enable advanced IoT and sensor devices that can be deployed on scale to collect increased environmental data for more predictive data/artificial intelligence modeling.

6.3.2. Green Chemistry

A key application of SMEC materials will be in enabling and driving clean chemistry. Over 95% of chemicals used in industry are made using catalysts,^[137] in addition to the aspirational application of catalysis to future fuel generation.^[101] Fundamentally, these catalysts often require external energy input in the form of electricity (electrocatalysis) or light (photocatalysis) to function. Yet, this external input is challenging to deliver in many applications. Recent work has shown that

M → E energy harvesting^[14,95,138] and ferroelectric materials^[118] can directly activate catalysts and eliminate the need for externally applied active energy inputs. SMEC materials can combine these phenomena and capture different types of energy to provide an “adaptive” catalyst that functions for a significantly expanded timespan. Notably, many-layered 2D crystals proposed as SMEC materials are also known to possess catalytically active facets for both pollutant degradation and future fuel production. These concepts mean that the proposed SMEC materials can be activated as catalysts by either motion, heat, or light without losses caused by connecting to an external circuit.

6.3.3. Quantum Data Storage

The final highlight is a blue-sky application for SMEC materials. Recently, the use of layered 2D crystals for heterogenous electronics and quantum data storage has been highlighted by Lemme et al.^[16] SMEC materials based on layered 2D crystals have potential use as an independently switchable memory based on thermal, photonic, or electronic stimuli. Alternatively, the energy absorption of SMEC materials across M, P, and T can potentially enable these materials to screen undesired energy that could influence the qubit. Similar to catalysis, layered 2D crystals have themselves already been identified as potential qubits;^[139] integrating a vdWs SMEC material into a qubit would allow direct integration of a screening material without undesired information loss and energy transfer. This application in quantum computing will take much more research to realize but the potential of SMEC materials to play a unique role in this field is clear.

6.4. Enabling Electronic Devices from SMEC Materials

While SMEC materials can provide exceptional improvements in captured ambient energy, transferring this energy to power a device is a critical process. Energy harvesters require both rectification and regulation of the output power supply and, therefore, in electronic devices, require integration with energy storage devices. Notably, if we use SMEC materials to drive catalytic systems, this integration can be eliminated, as discussed in Section 6.3. Integration into energy storage devices is intrinsically challenging for energy harvesting systems simply due to the different time domains of energy conversion processes. The most commonly used energy storage devices in existing electronics, the lithium-ion battery, requires ion diffusion and intercalation—a significantly slower process compared to the rapid voltage/charge generation from ambient energy harvesting. Integration with supercapacitors, particularly fast charging nanofluidic supercapacitors, could address this challenge;^[140] however, this needs strong validation in practice.

Furthermore, the realization that the connection of a SMEC material to an energy storage device fundamentally applies an electrical load onto the material is important. We have discussed how critical understanding the energy interplay in materials is, and this electrical load will influence the energy harvesting performance of the SMEC itself. Thus, a holistic approach to integrated harvester-storage systems is required, where the energy

demand of the energy storage device is matched to a given SMEC material for optimal energy transfer and storage.

The literature of individual energy harvesting materials can elucidate solutions to this challenge, with several innovative approaches being proposed. Yuan et al.^[141] described the macroscale design of external circuitry consisting of a rectifying bridge, dielectric capacitor, and integrated circuit, enabling the charging of a lithium-ion battery from an M → E energy harvester. This is a traditional and effective approach to capturing this energy, although it requires a significantly large footprint for the associated electronics compared to the active system. Particularly for wearable and implantable electronics, this large footprint is undesirable so alternative approaches are needed. Notably for low power requirement systems, if the energy harvesting (or SMEC) system enables a smaller energy storage device (i.e., the change from a pouch battery cell to a coin cell), no increase in electronic footprint would be required.

Vertically integrating energy harvesting and conversion systems into energy storage devices provides a direct pathway to achieve both low-loss energy storage and rectification to minimize overall device footprint.^[142–145] While exploring the options for coupling SMECs to energy storage devices is imperative, it is beyond the scope of this perspective, and the authors direct readers to a comprehensive review of options in this area by Pu, Hu, and Wang.^[146]

Layered 2D SMEC materials will provide two advantages for the coupling to energy storage devices compared to materials relying on individual energy inputs; 1) a significantly higher charge generation enabling faster charging of energy storage devices and, thus, reduced consequential parasitic losses; and 2) the ability to vdWs stack key components of energy storage devices, including metallic films and graphite electrodes, decreasing the energy barrier for charge transport from the SMEC material to the energy storage device. Thus, building vdWs heterostructures would allow for the integration of rectification diodes^[147] into energy storage devices, providing a pathway to device application that is not possible with non-layered 2D crystals.

7. Conclusions

Harvesting energy simultaneously from multiple varying energy sources is critical for an energy-efficient future. Layered 2D crystals, with their unique properties, sit at the interface of optical, thermal, and mechanical energy harvesting, and present a promising class of materials for advanced energy harvesting and bespoke SMEC materials. Clearly, each energy conversion mechanism influences the others during energy harvesting—and a thorough understanding of each energy conversion mechanism and its interactions at the molecular level is required to deconvolute and explain experimental observations. This interplay of energy conversion mechanisms, while complex and in the nascent stages of understanding, provides an opportunity for the development of materials with unprecedented performance in harvesting environmental and ambient energy. The combination of layered 2D crystals with SMEC functionality will enable the fabrication of high-performance devices, with applications ranging from wearable

electronics to green chemistry, from photovoltaics to quantum computing. Building vdWs heterostructures from these SMEC materials will enable direct coupling to energy storage and electronic devices, minimizing parasitic current losses common in integrating such devices together. Energy conversion processes are complicated and powerful systems—it is critical to understand the energy interplay network to design materials and devices that can fully exploit the interconnected nature of this energy landscape.

Acknowledgements

A.C. and P.C.S. contributed equally to this work. The authors gratefully acknowledge the financial support of the Australian Government through the Australian Research Council (ARC DP200101217). P.S. would like to acknowledge support from the Elizabeth & Vernon Puzey Fellowship at The University of Melbourne.

Open access publishing facilitated by The University of Melbourne, as part of the Wiley - The University of Melbourne agreement via the Council of Australian University Librarians.

Conflict of Interest

The authors declare no conflict of interest.

Keywords

2D materials, energy harvesting, ferroelectrics, photovoltaics, thermoelectrics

Received: April 29, 2022

Revised: June 6, 2022

Published online: August 2, 2022

- [1] C. Xu, Y. Song, M. Han, H. Zhang, *Microsyst. Nanoeng.* **2021**, *7*, 25.
 [2] S. Cao, J. Li, *Adv. Mech. Eng.* **2017**, *9*, 1687814017696210.
 [3] N. A. Shepelin, P. C. Sherrell, E. Goudeli, E. N. Skountzos, V. C. Lussini, G. W. Dicoski, J. G. Shapter, A. V. Ellis, *Energy Environ. Sci.* **2020**, *13*, 868.
 [4] N. A. Shepelin, V. C. Lussini, P. J. Fox, G. W. Dicoski, A. M. Glushenkov, J. G. Shapter, A. V. Ellis, *MRS Commun.* **2019**, *9*, 159.
 [5] P. C. Sherrell, A. Sutka, N. A. Shepelin, L. Lapčinskis, O. Verners, L. Germane, M. Timusk, R. A. Fenati, K. Mālnieks, A. V. Ellis, *ACS Appl. Mater. Interfaces* **2021**, *13*, 44935.
 [6] K. Roy, P. Devi, P. Kumar, *Nano Energy* **2021**, *87*, 106119.
 [7] Y. Bai, H. Jantunen, J. Juuti, *Adv. Mater.* **2018**, *30*, 1707271.
 [8] A. A. Khan, A. Mahmud, D. Ban, *IEEE Trans. Nanotechnol.* **2019**, *18*, 21.
 [9] M. Han, X. Chen, B. Yu, H. Zhang, *Adv. Electron. Mater.* **2015**, *1*, 1500187.
 [10] X. Chen, M. Han, H. Chen, X. Cheng, Y. Song, Z. Su, Y. Jiang, H. Zhang, *Nanoscale* **2017**, *9*, 1263.
 [11] L. Lapčinskis, K. Mālnieks, A. Linarts, J. Blūms, K. n. Šmits, M. Järvekūlg, M. r. Knite, A. Šutka, *ACS Appl. Energy Mater.* **2019**, *2*, 4027.
 [12] L. Pan, S. Sun, Y. Chen, P. Wang, J. Wang, X. Zhang, J.-J. Zou, Z. L. Wang, *Adv. Energy Mater.* **2020**, *10*, 2000214.
 [13] S. Li, Z. Zhao, J. Zhao, Z. Zhang, X. Li, J. Zhang, *ACS Appl. Nano Mater.* **2020**, *3*, 1063.
 [14] K. Wang, C. Han, J. Li, J. Qiu, J. Sunarso, S. Liu, *Angew. Chem., Int. Ed.* **2022**, *61*, e202110429.
 [15] L. Vannucci, U. Petralanda, A. Rasmussen, T. Olsen, K. S. Thygesen, *J. Appl. Phys.* **2020**, *128*, 105101.
 [16] M. C. Lemme, D. Akinwande, C. Huyghebaert, C. Stampfer, *Nat. Commun.* **2022**, *13*, 1392.
 [17] P. C. Sherrell, M. Fronzi, N. A. Shepelin, A. Corletto, D. A. Winkler, M. Ford, J. G. Shapter, A. V. Ellis, *Chem. Soc. Rev.* **2022**, *51*, 650.
 [18] F. Wang, Z. Wang, T. A. Shifa, Y. Wen, F. Wang, X. Zhan, Q. Wang, K. Xu, Y. Huang, L. Yin, C. Jiang, J. He, *Adv. Funct. Mater.* **2017**, *27*, 1603254.
 [19] N. Zhou, R. Yang, T. Zhai, *Mater. Today Nano* **2019**, *8*, 100051.
 [20] R. Roldán, L. Chirrolli, E. Prada, J. A. Silva-Guillén, P. San-Jose, F. Guinea, *Chem. Soc. Rev.* **2017**, *46*, 4387.
 [21] K. S. Novoselov, A. Mishchenko, A. Carvalho, A. H. C. Neto, *Science* **2016**, *353*, aac9439.
 [22] J. Qiu, H. Li, X. Chen, B. Zhu, H. Guo, F. Zhang, Z. Ding, L. Lang, J. Yu, J. Bao, *J. Appl. Phys.* **2021**, *129*, 125109.
 [23] J. Zhang, S. Jia, I. Kholmanov, L. Dong, D. Er, W. Chen, H. Guo, Z. Jin, V. B. Shenoy, L. Shi, J. Lou, *ACS Nano* **2017**, *11*, 8192.
 [24] A.-Y. Lu, H. Zhu, J. Xiao, C.-P. Chuu, Y. Han, M.-H. Chiu, C.-C. Cheng, C.-W. Yang, K.-H. Wei, Y. Yang, Y. Wang, D. Sokaras, D. Nordlund, P. Yang, D. A. Muller, M.-Y. Chou, X. Zhang, L.-J. Li, *Nat. Nanotechnol.* **2017**, *12*, 744.
 [25] L. Dong, J. Lou, V. B. Shenoy, *ACS Nano* **2017**, *11*, 8242.
 [26] V. K. Sangwan, M. C. Hersam, *Annu. Rev. Phys. Chem.* **2018**, *69*, 299.
 [27] P. Ajayan, P. Kim, K. Banerjee, *Phys. Today* **2016**, *69*, 38.
 [28] A. Chaves, J. G. Azadani, H. Alsalman, D. R. da Costa, R. Frisenda, A. J. Chaves, S. H. Song, Y. D. Kim, D. He, J. Zhou, A. Castellanos-Gomez, F. M. Peeters, Z. Liu, C. L. Hinkle, S.-H. Oh, P. D. Ye, S. J. Koester, Y. H. Lee, P. Avouris, X. Wang, T. Low, *npj 2D Mater. Appl.* **2020**, *4*, 29.
 [29] M.-J. Lee, J.-H. Ahn, J. H. Sung, H. Heo, S. G. Jeon, W. Lee, J. Y. Song, K.-H. Hong, B. Choi, S.-H. Lee, M.-H. Jo, *Nat. Commun.* **2016**, *7*, 12011.
 [30] T. Tan, X. Jiang, C. Wang, B. Yao, H. Zhang, *Adv. Sci.* **2020**, *7*, 2000058.
 [31] F. R. Fan, W. Wu, *Research* **2019**, *2019*, 7367828.
 [32] W. Li, J. Li, *Nat. Commun.* **2016**, *7*, 10843.
 [33] Y. Li, X. Wang, D. Tang, X. Wang, K. Watanabe, T. Taniguchi, D. R. Gamelin, D. H. Cobden, M. Yankowitz, X. Xu, J. Li, *Adv. Mater.* **2021**, *33*, 2105879.
 [34] D. J. Lacks, T. Shinbrot, *Nat. Rev. Chem.* **2019**, *3*, 465.
 [35] J. Li, N. A. Shepelin, P. C. Sherrell, A. V. Ellis, *Chem. Mater.* **2021**, *33*, 4304.
 [36] Z. L. Wang, A. C. Wang, *Mater. Today* **2019**, *30*, 34.
 [37] A. Šutka, K. Mālnieks, L. Lapčinskis, P. Kaufelde, A. Linarts, A. Bērziņa, R. Zābels, V. Jurkāns, I. Gorņevs, J. Blūms, M. Knite, *Energy Environ. Sci.* **2019**, *12*, 2417.
 [38] F. Li, T. Shen, C. Wang, Y. Zhang, J. Qi, H. Zhang, *Nano-Micro Lett.* **2020**, *12*, 106.
 [39] X. Guo, Y. Wang, A. J. Elbourne, A. Mazumder, C. Nguyen, V. Krishnamurthi, J. Yu, P. C. Sherrell, T. Daeneke, S. Walia, Y. Li, A. Zavabeti, *Nanoscale* **2022**, *14*, 6802.
 [40] S. Kim, M. K. Gupta, K. Y. Lee, A. Sohn, T. Y. Kim, K.-S. Shin, D. Kim, S. K. Kim, K. H. Lee, H.-J. Shin, D.-W. Kim, S.-W. Kim, *Adv. Mater.* **2014**, *26*, 3918.
 [41] S. Kim, T. Y. Kim, K. H. Lee, T.-H. Kim, F. A. Cimini, S. K. Kim, R. Hinchet, S.-W. Kim, C. Falconi, *Nat. Commun.* **2017**, *8*, 15891.
 [42] A. Šutka, P. C. Sherrell, N. A. Shepelin, L. Lapčinskis, K. Mālnieks, A. V. Ellis, *Adv. Mater.* **2020**, *32*, 2002979.

- [43] C. Chen, S. Zhao, C. Pan, Y. Zi, F. Wang, C. Yang, Z. L. Wang, *Nat. Commun.* **2022**, *13*, 1391.
- [44] A. G. Ricciardulli, P. W. M. Blom, *Adv. Mater. Technol.* **2020**, *5*, 1900972.
- [45] J. Zha, M. Luo, M. Ye, T. Ahmed, X. Yu, D.-H. Lien, Q. He, D. Lei, J. C. Ho, J. Bullock, K. B. Crozier, C. Tan, *Adv. Funct. Mater.* **2022**, *32*, 2111970.
- [46] L. Britnell, R. M. Ribeiro, A. Eckmann, R. Jalil, B. D. Belle, A. Mishchenko, Y.-J. Kim, R. V. Gorbachev, T. Georgiou, S. V. Morozov, A. N. Grigorenko, A. K. Geim, C. Casiraghi, A. H. C. Neto, K. S. Novoselov, *Science* **2013**, *340*, 1311.
- [47] Y. Li, A. Chernikov, X. Zhang, A. Rigosi, H. M. Hill, A. M. van der Zande, D. A. Chenet, E.-M. Shih, J. Hone, T. F. Heinz, *Phys. Rev. B* **2014**, *90*, 205422.
- [48] L. Mennel, V. Smejkal, L. Linhart, J. Burgdörfer, F. Libisch, T. Mueller, *Nano Lett.* **2020**, *20*, 4242.
- [49] L. Z. Tan, F. Zheng, S. M. Young, F. Wang, S. Liu, A. M. Rappe, *npj Comput. Mater.* **2016**, *2*, 16026.
- [50] R. von Baltz, W. Kraut, *Phys. Rev. B* **1981**, *23*, 5590.
- [51] V. M. Fridkin, *Crystallogr. Rep.* **2001**, *46*, 654.
- [52] J. E. Spanier, V. M. Fridkin, A. M. Rappe, A. R. Akbashev, A. Polemi, Y. Qi, Z. Gu, S. M. Young, C. J. Hawley, D. Imbrenda, G. Xiao, A. L. Bennett-Jackson, C. L. Johnson, *Nat. Photonics* **2016**, *10*, 611.
- [53] S. M. Young, A. M. Rappe, *Phys. Rev. Lett.* **2012**, *109*, 116601.
- [54] A. Zenkevich, Y. Matveyev, K. Maksimova, R. Gaynutdinov, A. Tolstikhina, V. Fridkin, *Phys. Rev. B* **2014**, *90*, 161409.
- [55] Y. Li, J. Fu, X. Mao, C. Chen, H. Liu, M. Gong, H. Zeng, *Nat. Commun.* **2021**, *12*, 5896.
- [56] I. Grinberg, D. V. West, M. Torres, G. Gou, D. M. Stein, L. Wu, G. Chen, E. M. Gallo, A. R. Akbashev, P. K. Davies, J. E. Spanier, A. M. Rappe, *Nature* **2013**, *503*, 509.
- [57] M. Qin, K. Yao, Y. C. Liang, *Appl. Phys. Lett.* **2008**, *93*, 122904.
- [58] S. Y. Yang, J. Seidel, S. J. Byrnes, P. Shafer, C. H. Yang, M. D. Rossell, P. Yu, Y. H. Chu, J. F. Scott, J. W. Ager, L. W. Martin, R. Ramesh, *Nat. Nanotechnol.* **2010**, *5*, 143.
- [59] A. M. Glass, D. v. d. Linde, T. J. Negran, *Appl. Phys. Lett.* **1974**, *25*, 233.
- [60] J. Liu, S. T. Pantelides, *Phys. Rev. Lett.* **2018**, *120*, 207602.
- [61] H. You, Y. Jia, Z. Wu, F. Wang, H. Huang, Y. Wang, *Nat. Commun.* **2018**, *9*, 2889.
- [62] J. Liu, S. T. Pantelides, *2D Mater.* **2019**, *6*, 025001.
- [63] K. Kanahashi, J. Pu, T. Takenobu, *Adv. Energy Mater.* **2020**, *10*, 1902842.
- [64] C. Wood, *Rep. Prog. Phys.* **1988**, *51*, 459.
- [65] Y. Liu, H. Wang, P. C. Sherrell, L. Liu, Y. Wang, J. Chen, *Adv. Sci.* **2021**, *8*, 2100669.
- [66] Y. Liu, S. Zhang, Y. Zhou, M. A. Buckingham, L. Aldous, P. C. Sherrell, G. G. Wallace, G. Ryder, S. Faisal, D. L. Officer, S. Beirne, J. Chen, *Adv. Energy Mater.* **2020**, *10*, 2002539.
- [67] L.-D. Zhao, S.-H. Lo, Y. Zhang, H. Sun, G. Tan, C. Uher, C. Wolverton, V. P. Dravid, M. G. Kanatzidis, *Nature* **2014**, *508*, 373.
- [68] V. Karthikeyan, S. L. Oo, J. U. Surjadi, X. Li, V. C. S. Theja, V. Kannan, S. C. Lau, Y. Lu, K.-H. Lam, V. A. L. Roy, *ACS Appl. Mater. Interfaces* **2021**, *13*, 58701.
- [69] A. Sood, C. Sievers, Y. C. Shin, V. Chen, S. Chen, K. K. H. Smithe, S. Chatterjee, D. Donadio, K. E. Goodson, E. Pop, *ACS Nano* **2021**, *15*, 19503.
- [70] S. Ghosal, S. Chowdhury, D. Jana, *ACS Appl. Mater. Interfaces* **2021**, *13*, 59092.
- [71] M. Xu, T. Liang, M. Shi, H. Chen, *Chem. Rev.* **2013**, *113*, 3766.
- [72] K. He, C. Poole, K. F. Mak, J. Shan, *Nano Lett.* **2013**, *13*, 2931.
- [73] S. B. Desai, G. Seol, J. S. Kang, H. Fang, C. Battaglia, R. Kapadia, J. W. Ager, J. Guo, A. Javey, *Nano Lett.* **2014**, *14*, 4592.
- [74] C. Lee, X. Wei, J. W. Kysar, J. Hone, *Science* **2008**, *321*, 385.
- [75] S. Bertolazzi, J. Brivio, A. Kis, *ACS Nano* **2011**, *5*, 9703.
- [76] J. Xia, J. Yan, Z. Wang, Y. He, Y. Gong, W. Chen, T. C. Sum, Z. Liu, P. M. Ajayan, Z. Shen, *Nat. Phys.* **2021**, *17*, 92.
- [77] S. Pak, J. Lee, Y.-W. Lee, A. R. Jang, S. Ahn, K. Y. Ma, Y. Cho, J. Hong, S. Lee, H. Y. Jeong, H. Im, H. S. Shin, S. M. Morris, S. Cha, J. I. Sohn, J. M. Kim, *Nano Lett.* **2017**, *17*, 5634.
- [78] S. Yang, Y. Chen, C. Jiang, *InfoMat* **2021**, *3*, 397.
- [79] D. Lloyd, X. Liu, J. W. Christopher, L. Cantley, A. Wadehra, B. L. Kim, B. B. Goldberg, A. K. Swan, J. S. Bunch, *Nano Lett.* **2016**, *16*, 5836.
- [80] J. Feng, X. Qian, C.-W. Huang, J. Li, *Nat. Photonics* **2012**, *6*, 866.
- [81] L. J. McGilly, A. Kerelsky, N. R. Finney, K. Shapovalov, E.-M. Shih, A. Ghiotto, Y. Zeng, S. L. Moore, W. Wu, Y. Bai, K. Watanabe, T. Taniguchi, M. Stengel, L. Zhou, J. Hone, X. Zhu, D. N. Basov, C. Dean, C. E. Dreyer, A. N. Pasupathy, *Nat. Nanotechnol.* **2020**, *15*, 580.
- [82] J. Jiang, Z. Chen, Y. Hu, Y. Xiang, L. Zhang, Y. Wang, G.-C. Wang, J. Shi, *Nat. Nanotechnol.* **2021**, *16*, 894.
- [83] Y. J. Zhang, T. Ideue, M. Onga, F. Qin, R. Suzuki, A. Zak, R. Tenne, J. H. Smet, Y. Iwasa, *Nature* **2019**, *570*, 349.
- [84] M.-M. Yang, D. J. Kim, M. Alexe, *Science* **2018**, *360*, 904.
- [85] L. Shu, S. Ke, L. Fei, W. Huang, Z. Wang, J. Gong, X. Jiang, L. Wang, F. Li, S. Lei, Z. Rao, Y. Zhou, R.-K. Zheng, X. Yao, Y. Wang, M. Stengel, G. Catalan, *Nat. Mater.* **2020**, *19*, 605.
- [86] A. M. Cook, B. M. Fregoso, F. de Juan, S. Coh, J. E. Moore, *Nat. Commun.* **2017**, *8*, 14176.
- [87] P. C. Sherrell, P. Palczynski, M. S. Sokolikova, F. Reale, F. M. Pesci, M. Och, C. Mattevi, *ACS Appl. Energy Mater.* **2019**, *2*, 5877.
- [88] F. M. Pesci, M. S. Sokolikova, C. Grotta, P. C. Sherrell, F. Reale, K. Sharda, N. Ni, P. Palczynski, C. Mattevi, *ACS Catal.* **2017**, *7*, 4990.
- [89] X. Yu, N. Guijarro, M. Johnson, K. Sivula, *Nano Lett.* **2018**, *18*, 215.
- [90] X. Yu, K. Sivula, *Curr. Opin. Electrochem.* **2017**, *2*, 97.
- [91] W. S. Yun, S. W. Han, S. C. Hong, I. G. Kim, J. D. Lee, *Phys. Rev. B* **2012**, *85*, 033305.
- [92] S. Yu, Q. Rice, B. Tabibi, Q. Li, F. J. Seo, *Nanoscale* **2018**, *10*, 12472.
- [93] M. R. Nellist, F. A. L. Laskowski, J. Qiu, H. Hajibabaei, K. Sivula, T. W. Hamann, S. W. Boettcher, *Nat. Energy* **2018**, *3*, 46.
- [94] A. Singh, G. Sharma, B. P. Singh, P. Vasa, *J. Phys. Chem. C* **2019**, *123*, 17943.
- [95] F. Bößl, I. Tudela, *Curr. Opin. Green Sustainable Chem.* **2021**, *32*, 100537.
- [96] W. Lauterborn, C.-D. Ohl, *Ultrason. Sonochem.* **1997**, *4*, 65.
- [97] S. Li, Z. Zhao, D. Yu, J.-Z. Zhao, Y. Su, Y. Liu, Y. Lin, W. Liu, H. Xu, Z. Zhang, *Nano Energy* **2019**, *66*, 104083.
- [98] Y. Chen, X. Deng, J. Wen, J. Zhu, Z. Bian, *Appl. Catal., B* **2019**, *258*, 118024.
- [99] G. Cheon, K.-A. N. Duerloo, A. D. Sendek, C. Porter, Y. Chen, E. J. Reed, *Nano Lett.* **2017**, *17*, 1915.
- [100] Q. Zhang, S. Zuo, P. Chen, C. Pan, *InfoMat* **2021**, *3*, 987.
- [101] L. Lin, P. Sherrell, Y. Liu, W. Lei, S. Zhang, H. Zhang, G. G. Wallace, J. Chen, *Adv. Energy Mater.* **2020**, *10*, 1903870.
- [102] S. V. Kalinin, V. Meunier, *Phys. Rev. B* **2008**, *77*, 033403.
- [103] T. Kistler, M. Y. Um, J. K. Cooper, I. D. Sharp, P. Agbo, *Energy Environ. Sci.* **2022**, *15*, 2061.
- [104] C. X. Lu, C. B. Han, G. Q. Gu, J. Chen, Z. W. Yang, T. Jiang, C. He, Z. L. Wang, *Adv. Eng. Mater.* **2017**, *19*, 1700275.
- [105] X. Wen, Y. Su, Y. Yang, H. Zhang, Z. L. Wang, *Nano Energy* **2014**, *4*, 150.
- [106] N. Sirica, P. P. Orth, M. S. Scheurer, Y. M. Dai, M. C. Lee, P. Padmanabhan, L. T. Mix, S. W. Teitelbaum, M. Trigo, L. X. Zhao, G. F. Chen, B. Xu, R. Yang, B. Shen, C. Hu, C. C. Lee, H. Lin, T. A. Cochran, S. A. Trugman, J. X. Zhu, M. Z. Hasan, N. Ni, X. G. Qiu, A. J. Taylor, D. A. Yarotski, R. P. Prasankumar, *Nat. Mater.* **2022**, *21*, 62.
- [107] X. Chen, Y. Zhao, F. Wang, D. Tong, L. Gao, D. Li, L. Wu, X. Mu, Y. Yang, *Adv. Sci.* **2022**, *9*, 2103957.
- [108] C. Jia, Y. Xia, Y. Zhu, M. Wu, S. Zhu, X. Wang, *Adv. Funct. Mater.* **2022**, *32*, 2201292.

- [109] P. Cheng, M. Ziegler, V. Ripka, H. Wang, K. Pollok, F. Langenhorst, D. Wang, P. Schaaf, *ACS Appl. Mater. Interfaces* **2022**, *14*, 15861.
- [110] Y. Yang, H. Zhang, G. Zhu, S. Lee, Z.-H. Lin, Z. L. Wang, *ACS Nano* **2013**, *7*, 785.
- [111] P. K. Tyagi, R. Kumar, Z. Said, *Nano Energy* **2022**, *93*, 106834.
- [112] M. K. Mohanta, A. Rawat, N. Jena, Dimple, R. Ahammed, A. De Sarkar, *ACS Appl. Mater. Interfaces* **2020**, *12*, 3114.
- [113] Z. Guan, H. Hu, X. Shen, P. Xiang, N. Zhong, J. Chu, C. Duan, *Adv. Electron. Mater.* **2020**, *6*, 1900818.
- [114] J. Shang, X. Tang, L. Kou, *Wiley Interdiscip. Rev.: Comput. Mol. Sci.* **2021**, *11*, e1496.
- [115] Đ. Dangić, S. Fahy, I. Savić, *npj Comput. Mater.* **2020**, *6*, 195.
- [116] S. Lee, S. Dursun, C. Duran, C. A. Randall, *J. Mater. Res.* **2011**, *26*, 26.
- [117] D. Sarkar, T. Ghosh, S. Roychowdhury, R. Arora, S. Sajan, G. Sheet, U. V. Waghmare, K. Biswas, *J. Am. Chem. Soc.* **2020**, *142*, 12237.
- [118] P. Abbasi, M. R. Barone, M. de la Paz Cruz-Jáuregui, D. Valdespino-Padilla, H. Paik, T. Kim, L. Kornblum, D. G. Schlom, T. A. Pascal, D. P. Fenning, *Nano Lett.* **2022**, *22*, 4276.
- [119] L. You, Y. Zhang, S. Zhou, A. Chaturvedi, S. A. Morris, F. Liu, L. Chang, D. Ichinose, H. Funakubo, W. Hu, T. Wu, Z. Liu, S. Dong, J. Wang, *Sci. Adv.* **2019**, *5*, eaav3780.
- [120] L. Niu, F. Liu, Q. Zeng, X. Zhu, Y. Wang, P. Yu, J. Shi, J. Lin, J. Zhou, Q. Fu, W. Zhou, T. Yu, X. Liu, Z. Liu, *Nano Energy* **2019**, *58*, 596.
- [121] S. Zhou, L. You, H. Zhou, Y. Pu, Z. Gui, J. Wang, *Front. Phys.* **2020**, *16*, 13301.
- [122] G. B. Osterhoudt, L. K. Diebel, M. J. Gray, X. Yang, J. Stanco, X. Huang, B. Shen, N. Ni, P. J. W. Moll, Y. Ran, K. S. Burch, *Nat. Mater.* **2019**, *18*, 471.
- [123] J. Junquera, P. Ghosez, *Nature* **2003**, *422*, 506.
- [124] W. Ding, J. Zhu, Z. Wang, Y. Gao, D. Xiao, Y. Gu, Z. Zhang, W. Zhu, *Nat. Commun.* **2017**, *8*, 14956.
- [125] S. Yuan, X. Luo, H. L. Chan, C. Xiao, Y. Dai, M. Xie, J. Hao, *Nat. Commun.* **2019**, *10*, 1775.
- [126] A. Belianinov, Q. He, A. Dziaugys, P. Maksymovych, E. Eliseev, A. Borisevich, A. Morozovska, J. Banys, Y. Vysochanskii, S. V. Kalinin, *Nano Lett.* **2015**, *15*, 3808.
- [127] J. R. Reimers, S. A. Tawfik, M. J. Ford, *Chem. Sci.* **2018**, *9*, 7620.
- [128] D. Lee, H. Lu, Y. Gu, S.-Y. Choi, S.-D. Li, S. Ryu, T. R. Paudel, K. Song, E. Mikheev, S. Lee, S. Stemmer, D. A. Tenne, S. H. Oh, E. Y. Tsybmal, X. Wu, L.-Q. Chen, A. Gruverman, C. B. Eom, *Science* **2015**, *349*, 1314.
- [129] K. Chang, J. Liu, H. Lin, N. Wang, K. Zhao, A. Zhang, F. Jin, Y. Zhong, X. Hu, W. Duan, Q. Zhang, L. Fu, Q.-K. Xue, X. Chen, S.-H. Ji, *Science* **2016**, *353*, 274.
- [130] B. Xu, H. Xiang, Y. Xia, K. Jiang, X. Wan, J. He, J. Yin, Z. Liu, *Nanoscale* **2017**, *9*, 8427.
- [131] Z. Fei, W. Zhao, T. A. Palomaki, B. Sun, M. K. Miller, Z. Zhao, J. Yan, X. Xu, D. H. Cobden, *Nature* **2018**, *560*, 336.
- [132] K. Yasuda, X. Wang, K. Watanabe, T. Taniguchi, P. Jarillo-Herrero, *Science* **2021**, *372*, 1458.
- [133] L. Ju, M. Bie, J. Shang, X. Tang, L. Kou, *J. Phys.: Mater.* **2020**, *3*, 022004.
- [134] A. Weston, E. G. Castanon, V. Enaldiev, F. Ferreira, S. Bhattacharjee, S. Xu, H. Corte-León, Z. Wu, N. Clark, A. Summerfield, T. Hashimoto, Y. Gao, W. Wang, M. Hamer, H. Read, L. Fumagalli, A. V. Kretinin, S. J. Haigh, O. Kazakova, A. K. Geim, V. I. Fal'ko, R. Gorbachev, *Nat. Nanotechnol.* **2022**, *17*, 390.
- [135] S. B. Lang, *Sourcebook of Pyroelectricity*, Vol. 2, CRC Press, Boca Raton, FL, USA **1974**.
- [136] J. F. Nye, *Physical Properties of Crystals: Their Representation by Tensors and Matrices*, Oxford University Press, Oxford, UK **1985**.
- [137] J. García-Serna, R. Piñero-Hernanz, D. Durán-Martín, *Catal. Today* **2022**, *387*, 237.
- [138] S. Tu, Y. Guo, Y. Zhang, C. Hu, T. Zhang, T. Ma, H. Huang, *Adv. Funct. Mater.* **2020**, *30*, 2005158.
- [139] X. Liu, M. C. Hersam, *Nat. Rev. Mater.* **2019**, *4*, 669.
- [140] J. Xiao, H. Zhan, X. Wang, Z.-Q. Xu, Z. Xiong, K. Zhang, G. P. Simon, J. Z. Liu, D. Li, *Nat. Nanotechnol.* **2020**, *15*, 683.
- [141] X. Yuan, X. Gao, J. Yang, X. Shen, Z. Li, S. You, Z. Wang, S. Dong, *Energy Environ. Sci.* **2020**, *13*, 152.
- [142] Y. Bai, H. Jantunen, J. Juuti, *Front. Mater.* **2018**, *5*, 65.
- [143] Y. R. Jeong, G. Lee, H. Park, J. S. Ha, *Acc. Chem. Res.* **2019**, *52*, 91.
- [144] Z. He, B. Gao, T. Li, J. Liao, B. Liu, X. Liu, C. Wang, Z. Feng, Z. Gu, *ACS Sustainable Chem. Eng.* **2019**, *7*, 1745.
- [145] M. B. Khan, H. Saif, Y. Lee, *Energies* **2020**, *13*, 1939.
- [146] X. Pu, W. Hu, Z. L. Wang, *Small* **2018**, *14*, 1702817.
- [147] B. Kim, J. Kim, P.-C. Tsai, H. Choi, S. Yoon, S.-Y. Lin, D.-W. Kim, *ACS Appl. Electron. Mater.* **2021**, *3*, 2601.



Alexander Corletto is currently a research fellow in electronic nanomaterials in the Department of Chemical Engineering at the University of Melbourne. His research involves the synthesis, manipulation, and characterization of novel nanomaterials and their heterostructures, aiming to discover optimized materials for energy applications including photovoltaics, piezoelectricity, photocatalysis, and others. He also has interest in the scalable manipulation and patterning of these nanomaterials for advanced device fabrication. He completed his Ph.D. research at the Australian Institute for Bioengineering and Nanotechnology at the University of Queensland, which involved investigating novel high-resolution patterning techniques for carbon nanotubes and nanomaterials



Amanda V. Ellis is the Head of the Chemical Engineering Department at the University of Melbourne, Australia. She has a Ph.D. (applied chemistry) from the University of Technology, Sydney. Her research focuses on 1D and 2D materials, polymer science, and energy storage/harvesting. She commenced as a lecturer at Flinders University, South Australia (2006), becoming a full professor (2013), an Australia Research Council Future Fellow (2014), and acting Associate Dean of Research for the Faculty of Science and Engineering (2016). In 2017 she joined the Department of Chemical Engineering at The University of Melbourne.



Nick A. Shepelin obtained his Bachelor of Science degree from Flinders University (2017) and his Ph.D. degree from the University of Melbourne (2020), graduating with the Chancellor's Prize for Excellence. He currently holds a position in the Laboratory for Multiscale Materials Experiments at the Paul Scherrer Institut as a Postdoctoral Fellow. His research focuses on interface, strain, and domain engineering of nonlinear dielectric materials, spanning from piezoelectricity and antiferroelectricity for robust and sustainable energy applications, to ferroelectricity for next-generation computing architectures. His research exploits a variety of material compositions, such as bulk polymers, 2D materials, and inorganic oxide thin films.



Marco Fronzi received his bachelor's/master's degree in physics in 2003, and his Ph.D. in computational material science in 2009 at University of Rome "Tor Vergata" (Italy). In 2010, he was awarded the Japan Society for the Promotion of Science Fellowship to conduct research at the National Institute for Materials Science (Japan). He has held positions with prestigious institutes, including Osaka University, University of Technology Sydney, and Tyndall National Institute. His interests lie in application of theoretical/computational methodologies, including quantum mechanical and ML models, for understanding/predicting properties of novel materials of technological interest.



David A. Winkler is a Professor at La Trobe University, Monash Institute for Pharmaceutical Sciences, and the University of Nottingham. He previously spent over 30 years at CSIRO researching the application of computational chemistry, AI, and ML methods to design of bioactive agents and materials. He has authored over 250 refereed journal articles and book chapters and 25 filed patents. He has won the CSIRO Medal for Business Excellence, RACI's Adrien Albert award for contributions to medicinal chemistry, the ACS Herman Skolnik award for excellence in cheminformatics, and a Royal Academy of Engineering (UK) Distinguished Fellowship (bioengineering).



Joseph G. Shapter obtained his Ph.D. from the University of Toronto in 1990. Until 1996, he worked at the University of Western Ontario (London, Ontario) and then moved to Flinders University and became Professor of Nanotechnology. In early 2018, he became the Pro Vice Chancellor (Research Infrastructure) at the University of Queensland and is a Senior Group Leader in the Australian Institute for Bioengineering and Nanotechnology (AIBN). The group makes nanomaterials and uses physical techniques to examine the properties of these systems. The work with carbon nanomaterials has seen these materials used for applications such as sensing and solar cells.



Peter C. Sherrell is an Elizabeth & Vernon Puzey Research Fellow and Chemical Engineering Teaching Fellow in the Department of Chemical Engineering at the University of Melbourne (2019–Present). He was awarded his Ph.D. in chemistry in 2012 from the University of Wollongong, and has since worked at Linköping University, Sweden (2013–2015) and as a Marie Skłodowska-Curie Individual Fellow at Imperial College London (2015–2018). His research bridges energy storage, conversion, and harvesting materials with a focus on engineering electronic, spatial, and chemical structure to enable improved material and device performance.